Development of a Two-Stream Mixing Layer from Tripped and Untripped Boundary Layers

James H. Bell*
NASA Ames/Stanford University, Stanford, California
and
Rabindra D. Mehta†
Stanford University, Stanford, California

A two-stream mixing layer with a velocity ratio of 0.6 was generated with two different initial conditions; one with both initial boundary layers laminar and one where both boundary layers were tripped. Some recent measurements have shown that relatively large spanwise variations can occur in the mean flow and turbulence properties of plane mixing layers, especially in the untripped case. Therefore, for the first time, all the data presented here were averaged over several spanwise locations. The results indicate that both the near- and far-field growth rates for the untripped case are significantly higher than for the tripped case. The maximum Reynolds stresses and higher order products for the two cases behave very differently in the near-field, but asymptote to approximately the same constant levels far downstream. The mean velocity and turbulence profiles in this region also collapse adequately for the two cases when plotted in similarity coordinates. The distance required to achieve self-similarity was found to be distinctly shorter for the tripped case, in contrast to previous observations. The higher growth rate for the untripped case is attributed to the presence of streamwise vortices, which result in additional entrainment by the mixing layer.

Nomenclature

C_f	= boundary-layer skin friction coefficient
H	= boundary-layer shape factor
r	= velocity ratio of the two streams, $= U_2/U_1$
Re_L	= Reynolds number, $= UL/\nu$
R_{uv}	= shear correlation coefficient, $= -\overline{u'v'}/\sqrt{\overline{u'^2}}\sqrt{\overline{v'^2}}$
U,V,W	= mean velocity in the X,Y,Z directions, respectively
U^*	= velocity parameter, $= (U - U_2)/(U_1 - U_2)$
U_0	= velocity difference, $= U_1 - U_2$
U_e	= freestream velocity in the wind tunnel
u',v',w'	= fluctuating velocity components in the X,Y,Z directions, respectively
u,v,w	= instantaneous velocity in the X,Y,Z directions, respectively, e.g., $u = U + u'$
X,Y,Z	= Cartesian coordinates for streamwise, normal, and spanwise directions, respectively
Y_0	= centerline of mixing layer (from error function fit)
$Y(N)$	= normal position where $U^* = N$
δ	= mixing layer width from error function fit
δ_{99}	= initial boundary-layer thickness
η	= similarity parameter $= (y-y_o)/\delta$
θ_0	= initial boundary-layer momentum thickness
$\overline{\quad}$	= (overbar) time-averaged quantity
$(\ )_{max}$	= maximum value at given X-station
$(\ )_1$	= value for high-speed side
$(\ )_2$	= value for low-speed side

*Post-Doctoral Fellow, Center for Turbulence Research.
†Senior Research Associate, Department of Aeronautics and Astronautics.

Introduction

TURBULENT mixing layers have been widely studied over the years, both in experiments and computations, for two main reasons. Firstly, mixing layers play an important role in many engineering applications. They govern the rate of mixing in combustion chambers and flow reactors and are also responsible for most of the noise generated by propulsion systems. Secondly, mixing layers are popular because their asymptotic behavior is thought to be quite simple in theory. For sufficiently high Reynolds numbers and downstream distance, Townsend[1] shows that the governing equations and boundary conditions for the plane turbulent mixing layer can yield "self-similar" solutions. The necessary conditions for self-similarity are that the mixing layer grows linearly and that the shapes of the mean velocity and turbulence profiles are independent of downstream distance when scaled by local mixing-layer thickness and velocity difference. The relationship between the maximum shear stress and the self-similar growth rate implied by the conservation of momentum is given by Townsend[1] for a two-dimensional mixing layer; it can be reduced to give

$$-\overline{u'v'}_{max}/U_0^2 = 0.141 d\delta/dX[(U_1 + U_2)/(U_1 - U_2)] \quad (1)$$

It is generally accepted that, after a sufficient development distance, all mixing layers achieve a self-similar condition. Although much attention has been directed toward determining the asymptotic spreading rate and turbulence properties of the self-similar plane mixing layer, many areas of confusion still remain.[2,3] The main reason for this confusion—or, more precisely, lack of agreement—between different experiments, is that mixing layers are very sensitive to small changes in their initial and operating conditions, the effects of which often persist for relatively long distances downstream. Amongst the parameters that are known to affect mixing-layer behavior are the splitter plate geometry,[4] the velocity ratio,[5,6] and the freestream turbulence intensity.[7] Another important parameter, which is the subject of the current study, is the state (laminar or turbulent) of the initial boundary layers. In spite of the theoretical arguments of Townsend,[1] it is not entirely clear from the available experimental data if the asymptotic mixing layer turbulence structure is indeed independent of the initial

boundary-layer state.[2,3] In addition, for two-stream mixing layers, there is very limited information on how the distance required to achieve a self-similar state is affected by the state of the initial boundary layers.

One of the first investigations in which the effects of initial conditions on mixing-layer development was studied was conducted by Bradshaw.[8] Bradshaw showed that a single-stream mixing layer achieved self-similarity in a distance equivalent to $1000\theta_0$, for both laminar and turbulent initial boundary layers. The asymptotic peak shear stress levels were slightly higher for the turbulent case, suggesting a higher asymptotic growth rate. Batt[9] and Hussain and Zedan[10] confirmed that the growth rate for a tripped single-stream mixing layer was indeed higher, although the peak streamwise fluctuation levels for the two cases were found to be comparable in the self-similar region. Hussain and Zedan's asymptotic profile shapes, plotted in their similarity coordinates, were different for the two cases because of the different growth rates. For both initial conditions, they suggested that the distance required for self-similarity in single-stream mixing layers decreased with increasing Re_{θ_0}, in contrast to Bradshaw's findings. For a given Re_{θ_0}, the case with a laminar initial boundary layer was found to achieve self-similarity in a shorter streamwise distance.

The situation for the two-stream mixing layer is even more complex. In contrast to the single-stream mixing layer, the asymptotic growth rate for the two-stream layer is found to be higher for the untripped case.[5,11-13] However, the asymptotic peak Reynolds stress levels, as well as the mean velocity and turbulence profiles, are found to be comparable for the two cases.[5,12] Thus, the applicability of Eq. (1), which uniquely relates the maximum shear stress to the growth rate (for a given velocity ratio), is called into question. In addition, no obvious criteria have emerged for the development distance required by two-stream mixing layers,[5] although various correlations based on the initial mixing layer momentum thick-

ness have been proposed.[12-14] The issue of the two-stream mixing-layer development is further complicated by the effects of velocity ratio and, for some cases, the presence and strong effects of the splitter plate wake.[6]

The present study was inspired by this rather odd dependence of mixing-layer behavior on the state of the initial boundary layers. Furthermore, some of our recent measurements made in a two-stream mixing layer originating from laminar boundary layers have shown that large spanwise variations occur in the mean flow and turbulence properties in the transition region.[15] The variations are caused by the presence of a relatively strong secondary vortex structure, consisting of counter-rotating pairs of streamwise vortices that ride among the primary spanwise rollers.[16] Some recent measurements in the mixing layer with the initial boundary layers tripped have indicated that such large-scale spanwise variations do not occur in this case. The main objectives of the present study are to document the effects of the initial boundary-layer state on the near- and far-field development of a two-stream mixing layer, and to try and relate the differences to the observed differences in structure.

Experimental Apparatus and Techniques

The experiments were conducted in a newly designed Mixing-Layer Wind Tunnel located in the Fluid Mechanics Laboratory at NASA Ames Research Center (Fig. 1). The wind tunnel consists of two separate legs that are driven individually by centrifugal blowers connected to variable speed motors. The two blower/motor combinations are sized such that one has three times the flow capacity of the other, although the components downstream of the wide-angle diffusers are identical on the two legs. The two streams are allowed to merge at the sharp edge of the tapered splitter plate. The included angle at the splitter plate edge, which extends 15 cm into the test section, is about 1 deg, and the edge
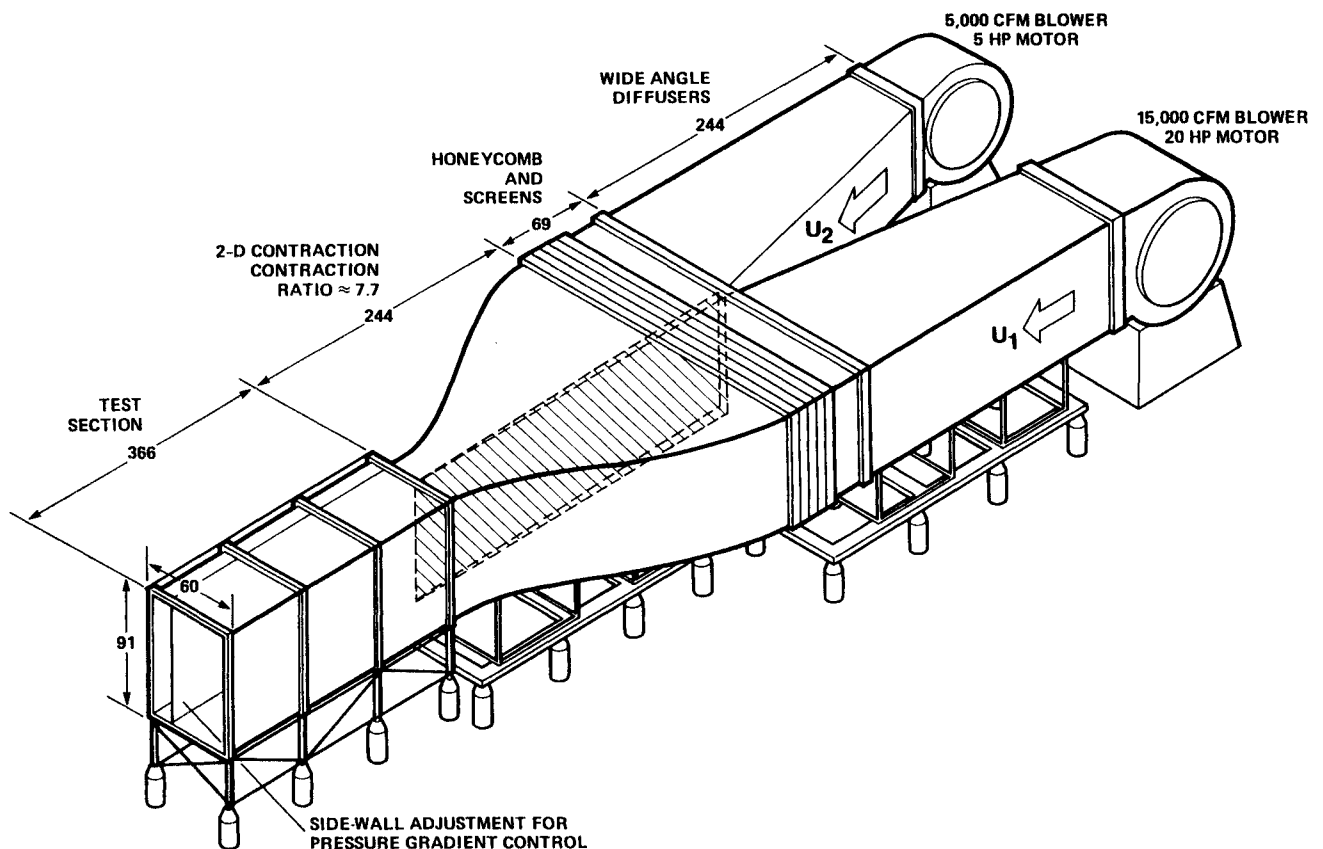

Fig. 1 Schematic of mixing-layer wind tunnel. Mixing layer is oriented vertically, and the adjustable sidewall is on the side facing away from the viewer.

Table 1 Initial boundary-layer properties

Condition	U_e, m/s	δ_{99}, cm	θ, cm	Re_θ	H	C_f $\times 10^3$
High-speed side, untripped	15.0	0.40	0.053	525	2.52	0.72
Low-speed side, untripped	9.0	0.44	0.061	362	2.24	0.91
High-speed side, tripped	15.0	0.76	0.082	804	1.49	5.30
Low-speed side, tripped	9.0	0.85	0.094	567	1.50	4.86

thickness is approximately 0.25 mm. The test section is 36 cm in the cross-stream direction, 91 cm in the spanwise direction, and 366 cm in length. One sidewall is slotted for probe access and flexible for pressure gradient control. For both the present sets of measurements, the flexible wall was adjusted to give a nominally zero streamwise pressure gradient.

For the present experiments, the leg driven by the bigger blower was operated at a freestream velocity in the test section of 15 m/s while the flow speed in the other leg was set at 9 m/s, thus giving a mixing layer with velocity ratio, $U_2/U_1 = 0.6$. The freestream velocities were typically found to remain constant to within 1% of the set value. At these operating conditions, the measured streamwise turbulence levels (u'/U_e) were about 0.15% and the transverse levels $(v'/U_e$ and $w'/U_e)$ were about 0.05%. The mean core flow was found to be uniform to within 0.5%, and cross-flow angles were less than 0.25 deg. Further details of the mixing-layer wind-tunnel design and calibration are given by Bell and Mehta.[17]

For the tripped cases, the boundary layers on the splitter plate were perturbed using round wire trips, about 0.75 mm diameter on the high-speed side and 1.2 mm diameter on the low-speed side. The wire trips were installed 15 cm upstream of the trailing edge to allow the boundary layers to recover from the perturbation. Details of the boundary layers measured at the splitter plate trailing edge are summarized in Table 1.

Measurements were made using a rotatable cross-wire probe held on a three-dimensional traverse and linked to a fully automated data acquisition and reduction system controlled by a Micro Vax II computer. The cross-wire probe had 5 μm diameter tungsten sensing elements about 1 mm long and positioned about 1 mm apart. The probe was calibrated statically in the potential core of the flow assuming a 'cosine-law' response to yaw, with the effective angle determined by calibration. The analog signals were low-pass filtered at 30 Khz to eliminate electronic noise, DC offset and amplified ($\times$ 10) before being fed into a computer interface. The interface contained a fast sample-and-hold A/D converter with 12 bit resolution and a multiplexer for connection to the computer.[18] Individual statistics were averaged over 5,000 samples obtained at a rate of 400 samples per second. (Note that this relatively low sampling rate does not affect the time-averaged data presented in this paper.)

Data were obtained in the uv- and uw-planes with a cross-wire probe at eight streamwise stations within the test section,

located between $X \sim$ 10 to 250 cm. The measurements of U, W, and $\overline{u'w'}$ were corrected for mean streamwise velocity gradient $(\partial U/\partial Y)$ effects assuming a linear variation in U between the cross-wire sensors.[15] The corrections were quite significant at the upstream stations, where the ratio of wire spacing to mixing-layer thickness was relatively large; for example, the correction factors for the secondary shear stress $(\overline{u'w'}/U_o^2)$ achieved levels equivalent to 40% of the measured values. The streamwise component of mean vorticity $(\omega_x = \partial W/\partial Y - \partial V/\partial Z)$ was computed using the central difference method. For both cases, data were obtained on cross-plane grids, typically consisting of 1200 points spaced at between 0.1 and 0.25 cm. All the data presented below were averaged over several spanwise locations. Typically, the data were averaged over a spanwise distance equivalent to about 30 mixing layer thicknesses at the first station, dropping to about three at the last measurement location. As an example of the spanwise variation of the measured quantities, the standard deviation of the maximum primary shear stress $(\overline{u'v'}_{max}/U_0^2)$ for the untripped case was about 40% at the first measurement station, dropping to about 6% at the last station; for the tripped case it was about 4% at all streamwise locations investigated.

Results and Preliminary Discussion

As suggested by Townsend,[1] the normalizing velocity scale is chosen as the velocity difference across the layer U_0 and the shear layer thickness δ is used to normalize the Y-coordinate. The shear-layer thickness is defined using a least-squares fit of the mean data to the error function profile shape:

$$U^* = [1 + erf(\eta)]/2 \tag{2}$$

Hence, the normalized Y-coordinate is defined by the similarity parameter:

$$\eta = (Y - Y_0)/\delta \tag{3}$$

where Y_0, the centerline of the mixing layer, is also defined from the error function fit. As discussed above, all the present measurements were spanwise-averaged in order to account for variations caused by the presence of streamwise vorticity in the mixing layer. At a given streamwise station, the measurements were obtained on a cross-plane grid. The grid was then divided into individual "slices" through the mixing layer, and the error function fit applied to each slice individually. The data in similarity coordinates were then averaged over all the slices to give a single spanwise-averaged profile.

The mean streamwise velocity profiles for the two cases are presented in Fig. 2. The solid lines represent Townsend's[1] error function relation [Eq. (2)]. Once past the near-field development region, the mean velocity profiles collapse quite well on the error function. In fact, the error function is generally a good approximation for the mean velocity distribution in most
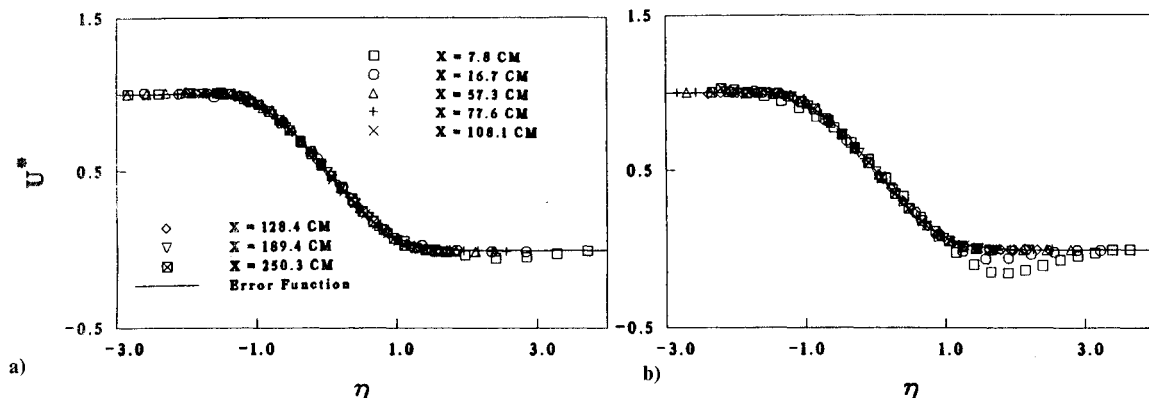

Fig. 2 Mean streamwise velocity profiles in similarity coordinates, at different streamwise stations; a) untripped (laminar) initial boundary layers, b) tripped (turbulent) initial boundary layers.

mixing layers, even when the mixing layer is highly perturbed.[19] This confirms, once again, that the behavior of the mean flow is a very weak indicator for assessing changes in the mixing-layer structure. Note the presence of a velocity defect

Fig. 3   Growth of mixing layer with increasing streamwise distance; □: untripped initial boundary layers, o: tripped initial boundary layers.

on the low-speed side in the profiles measured very close to the splitter plate trailing edge. The velocity defect is clearly seen at the first two measurement stations in the tripped case data and at the first station in the untripped data. The velocity defect, which is due to the splitter plate wake, is obviously bigger for the tripped case where the boundary layers are thicker. In both cases, the velocity defect is quickly "filled-in" by the mixing layer through entrainment, although the higher deficit in the tripped case lasts somewhat longer.

The streamwise growth of the mixing layer width, evaluated from the mean velocity profiles, is shown for both cases in Fig. 3. Initially, in the region very close to the splitter plate trailing edge ($X \leq 25$ cm), the mixing-layer thickness is obviously higher for the tripped case. Downstream of this region, the untripped case develops a distinctly higher growth rate compared to the tripped case. Further downstream ($X \geq 75$ cm), an approximately linear growth is indicated for both cases. In fact, the tripped case appears to exhibit a linear growth almost from the start. The difference in growth rates seems to persist, so that the asymptotic growth rate for the untripped case ($d\delta/dX = 0.023$), is distinctly higher than that for the tripped case ($d\delta/dX = 0.019$), in agreement with previous observations.[5,11-13] For the present results, the difference be-
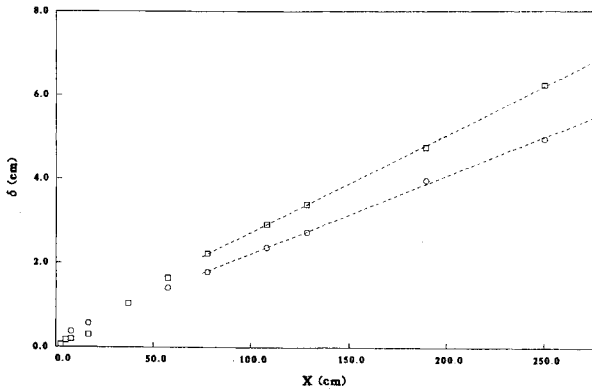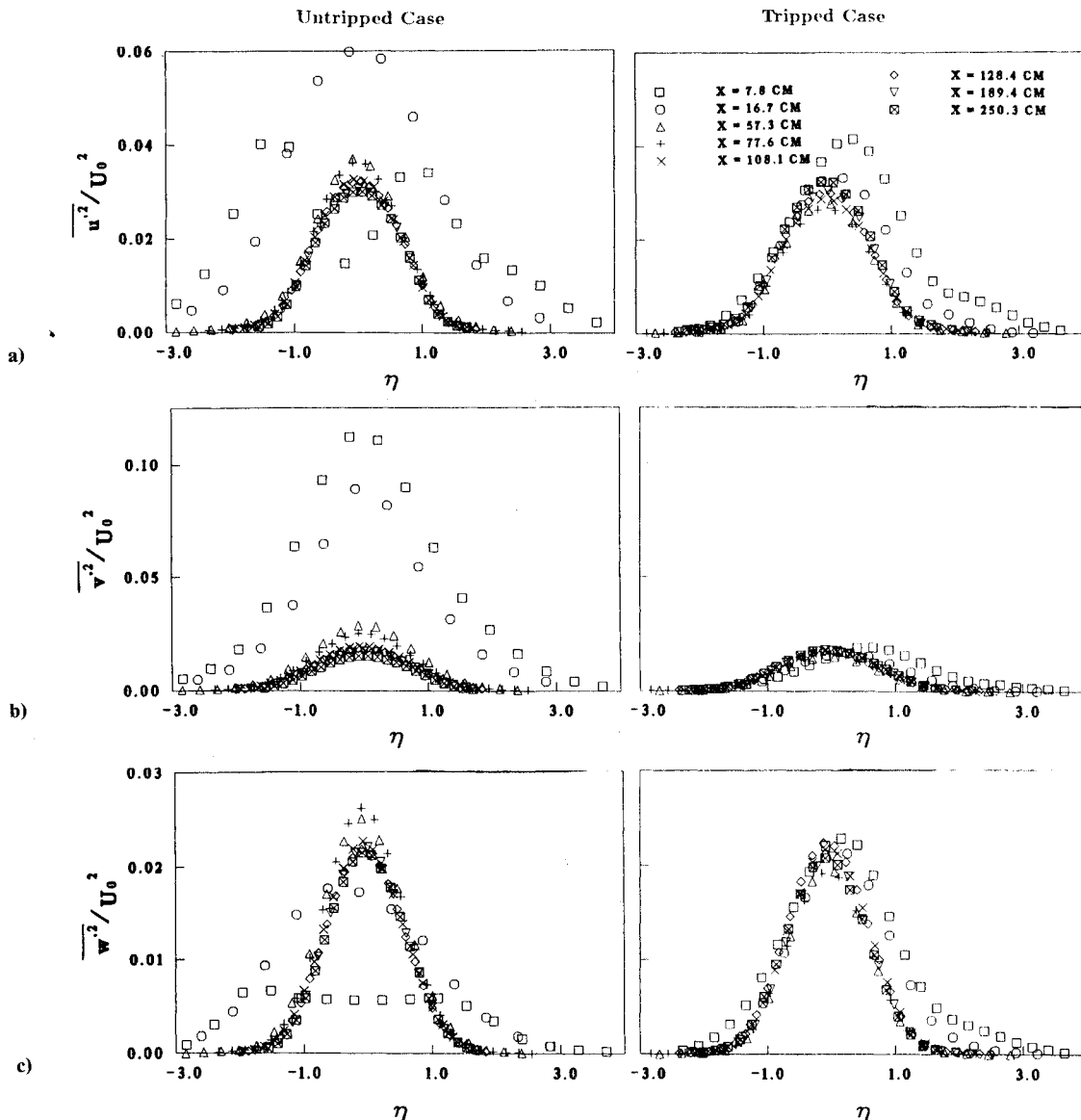

Fig. 4   Profiles of Reynolds normal stresses in similarity coordinates, at different streamwise stations. Case with untripped initial boundary layers is on the left, tripped initial boundary layers on the right. a) streamwise normal stress, $\overline{u'^2}$, b) cross-stream normal stress, $\overline{v'^2}$, c) spanwise normal stress, $\overline{w'^2}$.
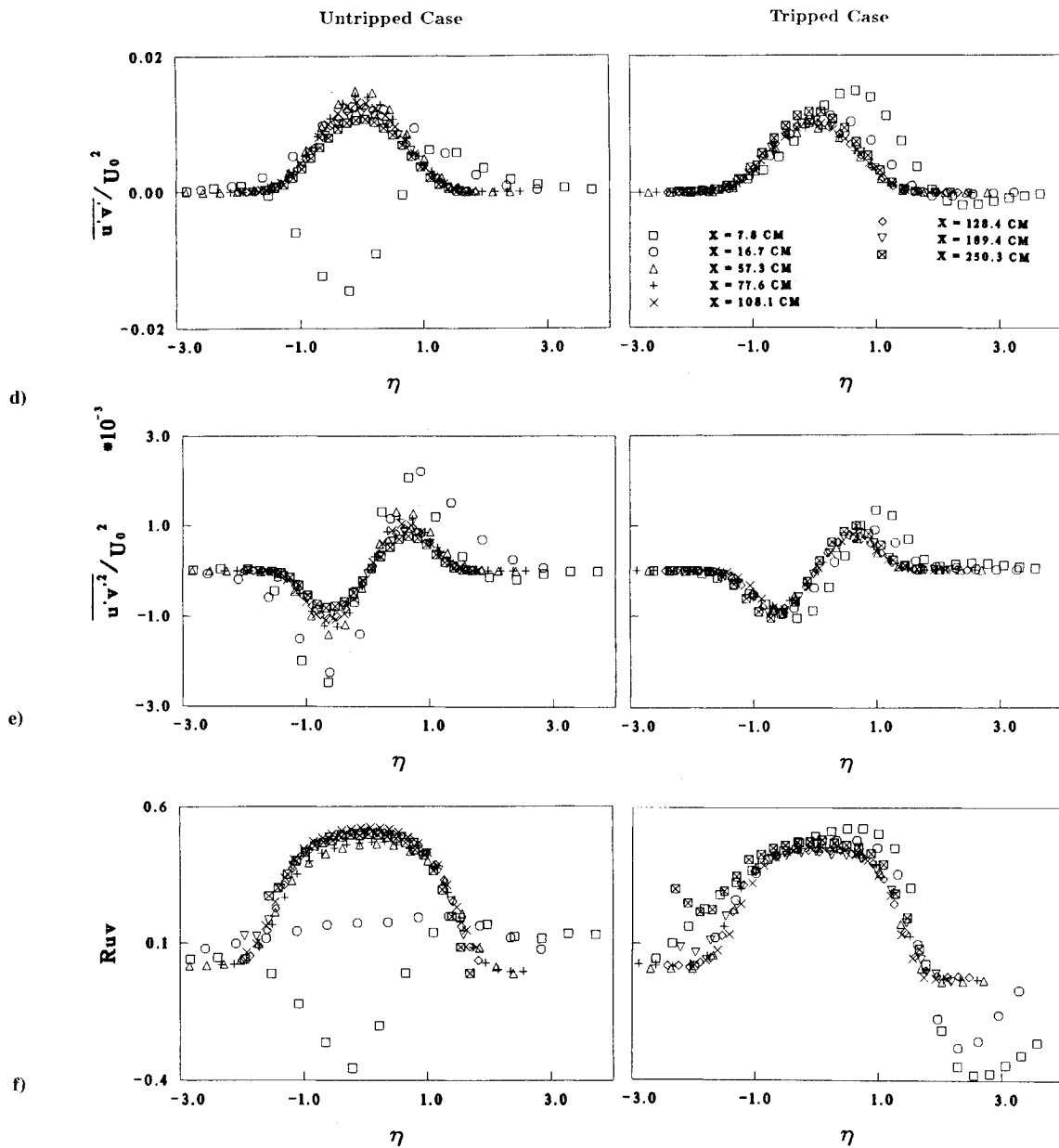
Fig. 4   (continued)   Profiles of turbulence products in similarity coordinates, at different streamwise stations. Case with untripped initial boundary layers is on the left, tripped initial boundary layers on the right. d) primary shear stress, $u'v'$, e) primary shear stress transport, $u'v'^2$, f) shear correlation coefficient, R_{uv}.

tween the two asymptotic growth rates is about 25%. However, the virtual origins for the two cases, obtained by extrapolating the linear regions, are not too dissimilar: $X_0 = -20$ cm for the untripped and $X_0 = -18$ cm for the tripped case. Note that whereas a linear growth of the mixing layer is a necessary condition for the achievement of self-similarity, it is by no means a sufficient one—the behavior of the turbulence quantities is critical in determining self-similarity.

The profiles for the three Reynolds normal stresses $(u'^2, v'^2,$ and $w'^2)$ for the two initial conditions are presented in Figs. 4a-c. For the tripped case data, the qualitative trends for all three normal stresses are similar. The maximum normal stress levels in the near-field are higher than the asymptotic level, with the distributions biased towards the low-speed side. There is also some indication of a secondary peak near the low-speed side edge of the mixing layer, coinciding with the region of mean velocity defect. The profile symmetry is recovered further downstream, and the profiles for all three normal stresses are found to collapse adequately beyond $X \sim 125$ cm. The untripped case data also show good collapse of the normal stress profiles beyond $X \sim 125$ cm, although the

near-field behavior is very different from the tripped case. In particular, the near-field levels of u'^2 and v'^2 are substantially higher than the asymptotic levels. The profiles are symmetric about the centerline from the beginning, although the first u'^2 profile has a curious double-peaked distribution.

The primary shear stress $(u'v')$ results for the two cases are presented in Fig. 4d. Once again, the initial tripped case profiles show higher levels and a bias towards the low-speed side. In addition, there is a negative shear stress peak towards the low-speed side edge of the layer. The first untripped case profile also shows a negative shear stress peak, but it is much stronger and is located towards the middle of the mixing layer. In both cases, the primary shear stress profiles also seem to show adequate collapse for $X \geq 125$ cm.

A more sensitive indicator for the achievement of self-similarity is the behavior of the higher order turbulence quantities that, in general, take longer to show asymptotic trends. The profiles for the triple product $(u'v'^2)$, which represents primary shear stress transport in the normal direction, are shown in Fig. 4e. In the tripped case, the first two profiles are again shifted towards the low-speed side and exhibit somewhat
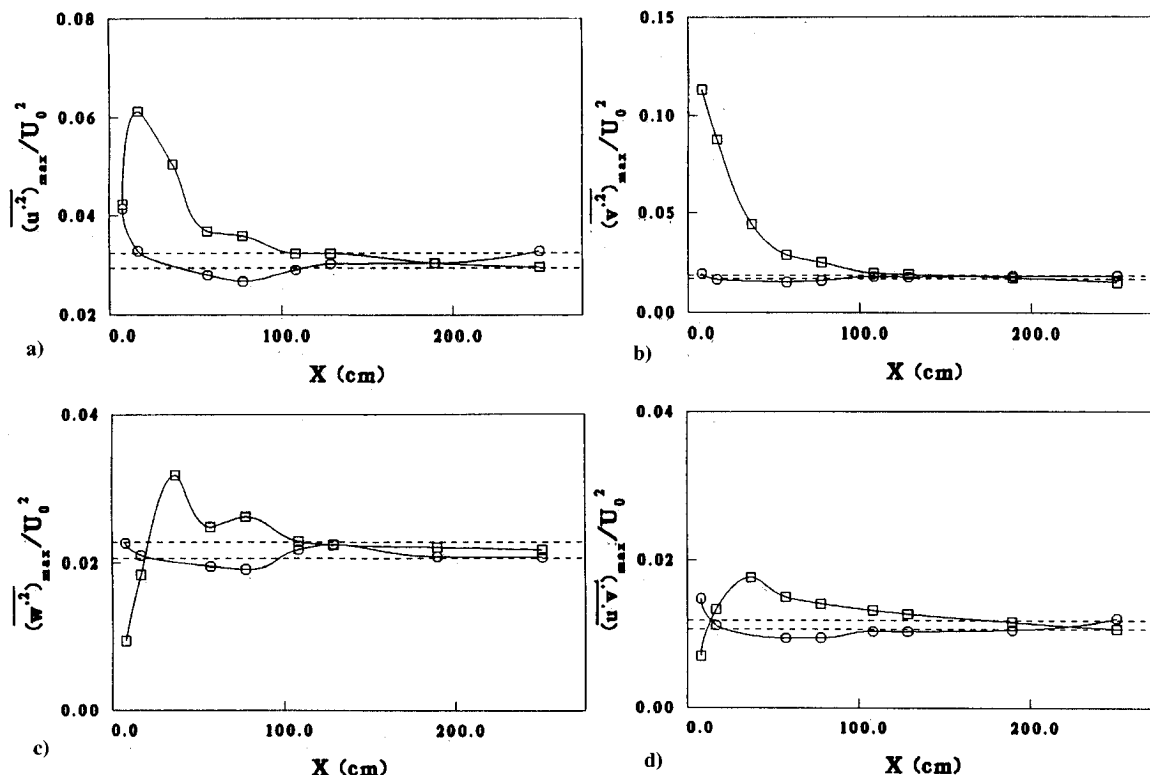
Fig. 5 Streamwise development of maximum level of turbulence products. □ : untripped initial boundary layers, o : tripped initial boundary layers, ---- ± 5% range around measured asymptotic level. a) streamwise normal stress, u'^2, b) cross-stream normal stress, v'^2, c) spanwise normal stress, w'^2, d) primary shear stress, $u'v'$.

higher levels than the asymptotic ones. In the untripped case, the initial levels are much higher, but the distributions are symmetric about the centerline. The results for both cases show a reasonable collapse of the profiles beyond $X \sim 125$ cm. The shear correlation coefficient (R_{uv}) profiles, which show changes in the mixing layer turbulence structure, are presented in Fig. 4f. The near-field results for both cases are qualitatively similar to those of the primary shear stress, as one would expect. However, in the far-field ($X \geq 125$ cm) the profiles for both cases display a more or less constant value of 0.5 over almost the whole width of the mixing layer, thus indicating that the mixing-layer turbulence has achieved an equilibrium state.

A more quantitative and direct comparison of the measured peak normal and primary shear stress levels for the two cases is given in Figs. 5a–d. For each initial condition, the qualitative trends for the four stresses are similar. The peak levels for the tripped case start out relatively high, drop to a minimum at $X \sim 75$ cm, and then rise slowly to the asymptotic levels. A more or less constant level is achieved by all the peak stresses for the tripped case beyond $X \sim 125$ cm. The untripped results all show a pronounced "overshoot" in the near-field region before dropping down to the asymptotic constant level. For all the peak stresses except v'^2, there is also a distinct peak exhibited at $X \sim 35$ cm. The normal stress peak levels have all reached constant levels beyond $X \sim 125$ cm. Furthermore, the asymptotic peak normal stress levels for the tripped and untripped cases are equal to within 10%—a band indicating a ± 5% region about the average asymptotic level is included in all these figures. The peak primary shear stress (Fig. 5d) for the tripped case also seems to have achieved a constant level by $X = 125$ cm. The peak primary shear stress for the untripped case exhibits a slow monotonic decrease beyond $X \sim 125$ cm, although by the last two measurement stations, the tripped and untripped peak levels also agree to within 10%.

As discussed above, organized (steady) streamwise vorticity, of scale comparable to the mixing-layer thickness, has been measured in the untripped case, but not in the mixing layer
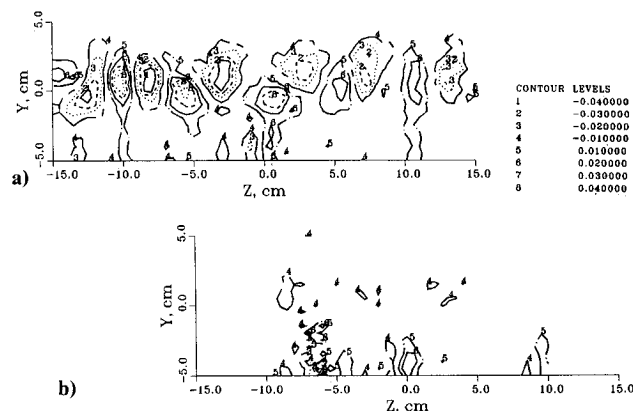

Fig. 6 Contours of mean streamwise vorticity in mixing layers at $X = 77.6$ cm. a) untripped initial boundary layers, b) tripped initial boundary layers. Plotted as $\omega_x/U_o(\text{cm}^{-1})$.

with the initial boundary layers tripped. Mean streamwise vorticity contours measured at one streamwise location ($X = 78$ cm) for the two cases are presented in Fig. 6. Streamwise vorticity, in counter-rotating pairs, is clearly seen in the results for the untripped case, whereas similar organized vorticity is absent for the tripped case. In principle, the state of the initial boundary layers should not matter, since the braid instability, responsible for the formation of the streamwise vorticity,[15] is present in both cases. However, in the tripped case, the instability presumably triggers off the (time-varying) boundary-layer turbulence, which would be expected to generate a wide range of (time-varying) vortex scales and strengths.

Our earlier work, with the initial boundary layers laminar, showed that for each organized steady streamwise vortex, a corresponding peak is produced in the secondary shear stress $(u'w')$, with the sign and strength correlated. The evolution of the streamwise vorticity can, therefore, be adequately monitored by observing the behavior of peak $u'w'$. The distribu-
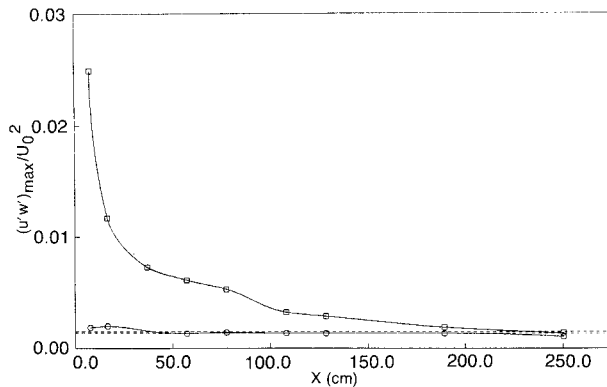
Fig. 7 Streamwise development of maximum level of secondary shear stress, $\overline{u'w'}$. □: untripped initial boundary layers, ○: tripped initial boundary layers, ---- ±5% range around measured asymptotic level.

tions of the peak averaged magnitudes of $\overline{u'w'}$ for the two cases are shown in Fig. 7. For a nominally two-dimensional mixing layer, $\overline{u'w'}$ should obviously have zero or very small values, as is the case for the tripped data, especially downstream of the first two measurement stations ($X \geq 50$ cm). However, for the untripped case, $\overline{u'w'}_{max}$ starts off at relatively high levels, followed by a rapid decay. By the last two measurement stations ($X \geq 175$ cm), $\overline{u'w'}_{max}$, for this case, has also achieved relatively low levels, comparable to the tripped case.

So all the measurements seem to indicate that the eventual (asymptotic) turbulence structure for the mixing layers with the initial boundary layers tripped and untripped is comparable, at least to within experimental accuracy.

Further Discussion

The contrasting near-field development for the tripped and untripped cases deserves additional discussion. In general, the behavior for both cases is comparable to that reported by Bradshaw[8] for the single-stream mixing layer. The untripped case has a very high growth rate and an overshoot in peak Reynolds stresses in the very near-field ($X \leq 50$ cm) development. This is due to the fact that with the untripped boundary layers, the initial velocity gradient ($\partial U/\partial Y$) is significantly higher, compared to the tripped case, since the boundary layers are thinner, and this leads to higher turbulence production, and, hence, growth rate, as suggested by Eq. (1). The levels for the tripped case, on the other hand, are found to increase slowly to the asymptotic level, after the initial drop downstream of the first station. The near-field levels in the present tripped case are a lot closer to the asymptotic levels than those reported by Bradshaw.[8] This difference was also observed in Mehta and Westphal's[6] measurements in a two-stream mixing layer and has been attributed to the effects of the splitter plate wake. The presence of the wake is clearly seen in the near-field velocity profiles as a velocity defect near the low-speed side edge of the mixing layer (Fig. 2). Apart from the velocity defect, which produces the secondary peaks in the Reynolds stresses, the effect of the wake is also to increase the velocity gradient across the mixing layer, which results in higher production of turbulence within the mixing layer. The bias in the Reynolds stress profiles towards the low-speed side is also caused by the wake and its associated effects. The wake effects are weaker in the untripped case, where the boundary layers are much thinner.

The peculiar double peak, seen in the first $\overline{u'^2}$ profile for the untripped case, is produced by the passage of spanwise vortex structures that are formed just upstream of this station. These structures tend to have a relatively quiescent core, with increased u activity at the periphery.[20] Such an effect is also seen in forced mixing layers, when spanwise vortices are inhibited from pairing so that well-aligned (two-dimensional) vor-

tices pass through the measurement domain.[19] The negative peak in $\overline{u'v'}$ and the large peak in $\overline{v'^2}$, seen at the first station, are caused by the same effect, and have also been observed in the forced mixing layer studies.[19,20] A similar effect is not observed at the first station in the tripped case, since the first spanwise vortex roll-up occurs further downstream, due to the thicker initial boundary layers. Also, with the initial boundary layers turbulent, the first roll-up and subsequent development may be expected to be more three-dimensional.[13] Note that, since the double-peak in the untripped $\overline{u'^2}$ distribution survives the spanwise averaging process, the initial development in this case is believed to be nominally two-dimensional. This notion is further supported by the fact that, at the first untripped station, the $\overline{v'^2}_{max}$ level is much higher than the asymptotic value, whereas the $\overline{w'^2}_{max}$ level is significantly lower.

Although the mixing-layer asymptotic growth rates appear to be different, each of the two cases studied here satisfies all three criteria defined above for the achievement of self-similarity, namely: linear growth, collapse of the mean flow and turbulence profiles when plotted in similarity coordinates, and asymptoting of the maximum Reynolds stresses to constant levels. As is often observed in turbulent shear flows, although the mean flow in both cases exhibits asymptotic behavior relatively early ($X \sim 75$ cm), the turbulence properties become self-similar somewhat later. The asymptotic peak levels of all five measured Reynolds stresses are comparable (within ±5%) for the two initial conditions. In addition, the mean flow and turbulence profile shapes for the two cases are also comparable in the self-similar region. All the results discussed so far are in qualitative agreement with those of Mehta and Westphal[5] and Browand and Latigo.[12] The results regarding the distance required for self-similarity, however, show new trends.

Based on the Reynolds shear stress results, in particular, the tripped case is assessed to be self-similar by $X = 125$ cm, whereas the untripped case does not achieve similarity until $X = 175$ cm. The relatively fast development of the tripped case is in contrast to observations in most of the previous studies.[6,8,10,12] Amongst the two-stream mixing-layer studies, Mehta and Westphal[5] found that the development distance for the two initial conditions was comparable, whereas Browand and Latigo[12] concluded that the laminar case had achieved similarity earlier. Browand and Latigo tripped only the high-speed side boundary layer, whereas in Mehta and Westphal's and the current study both boundary layers were tripped. The relatively fast development for this case is at least partly attributable to the effects of the splitter plate wake,[6] which increase the near-field Reynolds stress levels. On the other hand, the development of the untripped case is affected by the behavior of the streamwise vortical structures. So the present results suggest that in order to obtain a self-similar two-stream mixing layer in a relatively short distance, both initial boundary layers should be tripped.

The development distance for the two cases does not appear to follow any simple scaling. For example, the tripped case achieves self-similarity in a distance equivalent to about $1520\theta_{0_1}$, whereas the untripped case needs a distance equivalent to $1860\theta_{0_1}$. (Note that the initial mixing-layer momentum thickness is found to be equivalent to the high-speed side boundary-layer momentum thickness.[12-14]) In addition, the nondimensional development distances reported by Browand and Latigo[12] are significantly lower (by almost a factor of two) compared to those found in the present study. It is worth noting, though, that direct comparisons with previous work may not really be valid, since this is the first time that a spanwise averaging scheme has been employed.

Using the measured values for the growth rates, the maximum shear stress for a two-dimensional self-similar mixing layer can be predicted with Eq. (1). The measured and predicted values of the maximum primary shear stress are compared for the two initial conditions employed in the present study in Table 2.

Table 2 Maximum primary shear stress

Condition	Measured growth	Measured $\overline{u'v'}_{max}/U_0^2$	Predicted $\overline{u'v'}_{max}/U_0^2$	Percent difference
Tripped	0.019	0.011	0.0104	5%
Untripped	0.023	0.011	0.0131	−19%

While the measured and predicted values of the maximum primary shear stress for the tripped case look comparable, the prediction for the untripped case is clearly higher by a significant margin over the measurements. This discrepancy, though, may in fact help to explain the odd behavior of the untripped mixing layers. As stated above, Eq. (1) is really only applicable to two-dimensional mixing layers. As also discussed and shown above, plane mixing layers originating from laminar boundary layers are found to contain relatively strong, organized, and large-scale three-dimensionality in the form of streamwise vorticity.[15] It seems feasible that the increased large-scale (organized) three-dimensionality would lead to increased entrainment of the potential fluid and, hence, a higher growth rate. Note that these types of streamwise structures are found to ride over the spanwise vortices without significantly affecting the nominal two-dimensionality of the spanwise structures and their pairing process.[16] The main entrainment due to the spanwise structures is, therefore, maintained, and the streamwise structures provide additional entrainment. Some recent measurements by Plesniak and Johnston[21] in a curved mixing layer showed that the amplification of organized streamwise vorticity, through the Taylor-Görtler instability in their case, does indeed increase the growth rate of the mixing layer. Bell and Mehta's[15] measurements suggest that the strength of the streamwise vortices decays continuously with downstream distance, following a $1/X^{1.5}$ decay. By their last measurement station at $X = 250$ cm, the streamwise vortices were found to be extremely weak—to the extent that the mixing layer may be considered more or less two-dimensional. So it is possible that further downstream, the untripped mixing-layer growth rate may drop down to the tripped value, but this cannot be confirmed from the present measurements; the measurements could not be continued further downstream because of increasing interaction between the mixing layer and the sidewall boundary layers. The implication of the present conjecture is obviously that the untripped mixing layer would have two distinct linear growth regions. This is not a totally unfeasible expectation, especially since Hussain and Zedan[10] have already reported such a behavior in the development of a single-stream mixing layer. They also reported that the change in growth rate occurred rather abruptly, and so the fact that the present untripped growth rate does not appear to change towards the end of the measurement domain may not be too surprising.

The present results suggest that the current criteria for assessing self-similarity is not adequate and that a quantity parameterizing the effects of the three-dimensionality, such as the secondary shear stress ($\overline{u'w'}$), is also required. It is also apparent that the self-similar growth rate of a mixing layer will only be achieved once the shear stresses have reached asymptotic levels. This does not necessarily imply that the turbulence structure achieves self-similarity earlier compared to the mean flow. A longer streamwise extent of the mixing layer needs to be investigated in order to obtain the eventual asymptotic growth rate.

Conclusions

The effects of the state (laminar or turbulent) of the initial boundary layers on the development of a two-stream plane mixing layer, with a velocity ratio of 0.6, have been investigated experimentally. Spanwise-averaged profiles are compared, for the first time, since large spanwise variations in the mean flow and turbulence quantities have recently been measured, especially in the untripped case. At some point in the development, each case appeared to satisfy all three criteria for self-similarity, namely: linear growth, collapse of the

mean flow and turbulence profiles when plotted in similarity coordinates, and the invariance of the peak turbulence quantities with streamwise distance. For both cases, the mean flow appears to exhibit self-similarity a lot earlier than the turbulence quantities. In agreement with previous observations, the linear growth rate for the untripped case was found to be higher than that for the tripped case, by about 25% in the present results. The peak Reynolds stress data indicate that the tripped case achieves self-similarity faster ($X \sim 125$ cm), compared to the untripped case that exhibits self-similarity only towards the end of the measurement domain ($X \sim 175$ cm). The faster development of the tripped case is at least partly attributable to the effects of the splitter plate wake. The difference in development distance for the two cases cannot be accounted for through any simple scaling parameter, such as the mixing-layer initial momentum thickness. The asymptotic turbulence structure for the two cases compares extremely well in the self-similar region, to well within 10% for most of the peak Reynolds stresses and higher order products. The higher linear growth rate for the untripped case is attributed to the presence of three-dimensionality in the form of streamwise vortices, which would tend to increase entrainment and, hence, growth, of the mixing layer. The present Reynolds stress results indicate that, by the end of the measurement domain, the streamwise structures have decayed to the point where the untripped mixing layer structure is comparable to that of the tripped case. It is, therefore, proposed here that the growth rate of the untripped mixing layer will soon decrease to that of the tripped case, thus giving a single asymptotic growth rate for both initial conditions. Work is in progress to investigate this conjecture further.

References

[1]Townsend, A. A., *Structure of Turbulent Shear Flow*, Cambridge Univ. Press, Cambridge, England, 1976, pp. 188–230.

[2]Rodi, W., "A Review of Experimental Data of Uniform Density Free Turbulent Boundary Layers," *Studies in Convection*, Vol. 1, edited by B. E. Launder, Academic, London, England, 1975, pp. 79–165.

[3]Birch, S. F., and Eggers, J. M., "A Critical Review of the Experimental Data for Developed Free Turbulent Shear Layers," NASA SP-321, Jan. 1973.

[4]Dziomba, B., and Fiedler, H. E., "Effects of Initial Conditions on Two-Dimensional Free Shear Layers," *Journal of Fluid Mechanics*, Vol. 152, March 1985, pp. 419–442.

[5]Mehta, R. D., and Westphal, R. V., "Near-Field Turbulence Properties of Single- and Two-Stream Plane Mixing Layers," *Experiments in Fluids*, Vol. 4, Sept. 1986, pp. 257–266.

[6]Mehta, R. D., and Westphal, R. V., "Effect of Velocity Ratio on Plane Mixing Layer Development," *Proceedings of the Seventh Symposium on Turbulent Shear Flows*, Stanford Univ., Stanford, CA, Aug. 21–23, 1989, pp. 3.2.1–3.2.6.

[7]Patel, R. P., "Effects of Stream Turbulence on Free Shear Flows," *Aeronautical Quarterly*, Vol. 29, Feb. 1978, pp. 33–43.

[8]Bradshaw, P., "The Effect of Initial Conditions on the Development of a Free Shear Layer," *Journal of Fluid Mechanics*, Vol. 26, Oct. 1966, pp. 225–236.

[9]Batt, R. G., "Some Measurements on the Effect of Tripping the Two-Dimensional Shear Layer," *AIAA Journal*, Vol. 13, No. 2, 1975, pp. 245–247.

[10]Hussain, A. K. M. F., and Zedan, M. F., "Effects of the Initial Condition on the Axisymmetric Free Shear Layer: Effects of the Initial Momentum Thickness," *Physics of Fluids*, Vol. 21, July 1978, pp. 1100–1112.

[11]Oster, D., Wygnanski, I. J., and Fiedler, H. E., "Some Preliminary Observations on the Effect of Initial Conditions on the Structure of the Two-Dimensional Turbulent Mixing Layer," *Turbulence in Internal Flows*, edited by S. N. B. Murthy, Hemisphere, Washington, DC, 1977, pp. 67–87.

[12]Browand, F. K., and Latigo, B. O., "Growth of the Two-Dimensional Mixing Layer from a Turbulent and Nonturbulent Boundary Layer," *Physics of Fluids,* Vol. 22, June 1979, pp. 1011-1019.

[13]Browand, F. K., and Troutt, T. R., "The Turbulent Mixing Layer: Geometry of Large Vortices," *Journal of Fluid Mechanics,* Vol. 158, Sept. 1985, pp. 489-509.

[14]Ho, C.-M., and Huerre, P., "Perturbed Free Shear Layers," *Annual Review of Fluid Mechanics,* Vol. 16, March 1984, pp. 365-424.

[15]Bell, J. H., and Mehta, R. D., "Three-Dimensional Structure of a Plane Mixing Layer," AIAA Paper 89-0124, Jan. 1989. Also, Dept. of Aeronautics and Astronautics, Stanford Univ., JIAA Report TR-90, Stanford, CA, March 1989.

[16]Lasheras, J. C., Cho, J. S., and Maxworthy, T., "On the Origin and Evolution of Streamwise Vortical Structures in a Plane, Free Shear Layer," *Journal of Fluid Mechanics,* Vol. 172, Nov. 1986, pp.

231-258.

[17]Bell, J. H., and Mehta, R. D., "Design and Calibration of the Mixing Layer Wind Tunnel," Dept. of Aeronautics and Astronautics, Stanford Univ., JIAA Report TR-89, Stanford, CA, May 1989.

[18]Westphal, R. V., and Mehta, R. D., "Crossed Hot-Wire Data Acquisition and Reduction System," NASA TM-85871, Jan. 1984.

[19]Mehta, R. D., Inoue, O., King, L. S., and Bell, J. H., "Comparison of Experimental and Computational Techniques for Plane Mixing Layers," *Physics of Fluids,* Vol. 30, No. 7, 1987, pp. 2054-2062.

[20]Oster, D., and Wygnanski, I. J., "The Forced Mixing Layer Between Two Parallel Streams," *Journal of Fluid Mechanics,* Vol. 123, Oct. 1982, pp. 91-130.

[21]Plesniak, M. W., and Johnston, J. P., "Reynolds Stress Evolution in Curved Two-Stream Mixing Layers," *Proceedings of the Seventh Symposium on Turbulent Shear Flows,* Stanford Univ., Stanford, CA, Aug. 21-23, 1989, pp. 6.3.1-6.3.6.